NUMERICAL SIMULATION OF THE TURBULENT TRANSITION IN FREE ROUD JETS

Ana Marta de Souza
School of Mechanical Engineering - Federal University of Uberlandia – Av. João Naves de Ávila, 2160 – Uberlândia – Brasil.
amsouza@mecanica.ufu.br

Francisco José de Souza
School of Mechanical Engineering - Federal University of Uberlandia – Av. João Naves de Ávila, 2160 – Uberlândia – Brasil.
fjsouza@mecanica.ufu.br

Aristeu da Silveira Neto
School of Mechanical Engineering - Federal University of Uberlandia – Av. João Naves de Ávila, 2160 – Uberlândia – Brasil.
aristeus@mecanica.ufu.br

Abstract. *The interest in jet flows is justified by their remarkable technological importance in industrial applications, aircraft propulsion systems and noise generation processes. In all these applications, jet control is the key for the optimization of processes or even the solution of specific problems. The present work consists in the physical analysis of free round jets by means of three-dimensional simulations. Besides this goal, analyses of the influence of different types of perturbations on the formation and evolution of turbulent structures are sought. From the point of view of physical analysis, successful results were obtained by using the code SPECTRAL, with which Direct Numerical Simulations were run using a pseudo-spectral method. The results of these simulations allowed to evidence structures and phenomena typical of the flows investigated, as well as to better understand the respective generation mechanisms. The possibility of controlling the jet through the imposition of different perturbations to the initial conditions could also be confirmed. The proximity of the inertial region to the inclination of -5/3 and the decay region were verified in the energy spectra.*

Keywords*: round jets, simulation of turbulent transition, pseudo-spectral method.*

1. Introduction

The turbulence in jets has been widely studied numerical and experimentally. The interest in this type of flow is justified due its considerable technological importance. The industrial applications involve mixing processes, heat transfer, lubrification and tahw, fuel injection in combustion cameras, propulsion systems of aircrafts and airplanes. The optimization of these processes may be obtained through the jet control. This control can be performed through the manipulation of the coherent structures, which are responsible to influence strongly the jet dynamic, especially on transition region near the inlet nozzle.

The jet control application on noise reduction is particular relevant, because it is recognized that the vortex pairings constitute an important source of noise generation. Both passive and active control can be used to modify the jet dynamics. The passive control refers to control of the jet spatial evolution through the use of particular shapes of the inlet nozzle (Gutmark e Gristein, 1999). The active control refers to deterministic perturbation at the jet inlet created through energy consuming devices, which can be obtained, in practice, through the use of loud-speakers (Crow and Champagne, 1971; Zaman and Hussain,1980) or flap actuator (Zaman et al, 1994; Suzuki et al., 2000).

Besides the applications mentioned, the turbulent jet is a simple canonical flow quite important in the physic point of view. This flow serves as simple model for more complex flows.

A better comprehension on the formation and evolution of the flow allows an effective control over jets for different industrial interests, as well as contribute for refinement of theories and models already existent for the description of turbulent flows. Despite many manuscripts of literature approach the subject, many of them restrict to comparisons of average behavior. Some of them show the typical structures over some specified conditions. Therefore, there is lack of vortex structures understanding, initial conditions influence and different perturbations over the jet formation and evolution.

The main goal of this work is to perform the physical analysis of jet flows. To reach this goal, three-dimensional numerical simulations were performed using a method pseudo-spectral and analysis of the influence of two different kinds of inlet perturbations over the formation and evolution of vortex structures was carried out.

2. Governing Equations and Numerical Method

The Navier-Stokes and continuity equations with unit physical properties that describe the incompressible jet flow are:

$$\begin{cases} \dfrac{\partial u_i}{\partial t} + \dfrac{\partial}{\partial x_j}\left(u_i u_j\right) = -\dfrac{\partial p}{\partial x_i} + \dfrac{\partial^2 u_i}{\partial x_j \partial x_j} \\ \dfrac{\partial u_i}{\partial x_i} = 0 \end{cases} \tag{1}$$

The governing equations can be written in the spectral space:

$$\begin{cases} \dfrac{\partial \hat{u}_\ell}{\partial t} + \nu\, k^2 \hat{u}_\ell = -ik_m P_{jm}\left(\vec{k}\right) \displaystyle\int_{\vec{p}+\vec{q}=\vec{k}} \hat{u}_\ell\left(\vec{p}\right)\hat{u}_j\left(\vec{q}\right) d\vec{p} \\ i\vec{k}\cdot\hat{\vec{u}} = 0 \end{cases} \tag{2}$$

The Navier-Stokes equations do not dependent of the pressure concept in Fourier space, contrary to what happens in the physical space. The resolution of non-linear convolution integral that appears on Eq. (2) is impracticable due to its high computational cost. For this reason, the methods named pseudo-spectral have been used. These methods consist in solving the product of velocities in physical space and transforming them to Fourier space, in which the derivatives are computed. Thus, the transformed velocity field is computed, the inverse transform calculated and the velocity field in the physical space determined.

The SPECTRAL code, which was developed by the authors, employees a pseudo-spectral method to solve the Navier-Stokes equations in spectral space, which can be rewritten in the following form for the three flow directions:

$$\frac{\partial \hat{u}}{\partial t} = -\hat{H}_{u_\pi} + \nu\left(-k_x^{\,2} - k_y^{\,2} - k_z^{\,2}\right)\hat{u}\,, \tag{3}$$

$$\frac{\partial \hat{v}}{\partial t} = -\hat{H}_{v_\pi} + \nu\left(-k_x^{\,2} - k_y^{\,2} - k_z^{\,2}\right)\hat{v} \tag{4}$$

$$\frac{\partial \hat{w}}{\partial t} = -\hat{H}_{u_\pi} + \nu\left(-k_x^{\,2} - k_y^{\,2} - k_z^{\,2}\right)\hat{w}\,, \tag{5}$$

where $\hat{u}$, $\hat{v}$ e $\hat{w}$ are the Fourier coefficients for the velocities *u*, *v* e *w*, respectively; and $\hat{H}_{u_\pi}$, $\hat{H}_{v_\pi}$ e $\hat{H}_{w_\pi}$ represent the advective terms in each equation projected into the π plane.

Equations (3), (4) and (5) were advanced in time with the Adams-Bashforth and Runge-Kutta schemes, both of 3nd order. After the two initial time steps with the 3rd-order Runge Kutta scheme (RK3), the temporal advance employs the 3rd-order Adams Bashforth scheme (AB3). At each time step or sub-step the transformed Navier-Stokes equations are solved.

At the moment, only periodic boundary conditions are available in the SPECTRAL code.

2.1. Initial Conditions

The jet flow simulations were performed at Reynolds number 1600, time step 0.0025 s and 120^3 Fourier modes in a cubic domain of dimensions *8R x 8R x 8R*, where *R* is the initial radius, as shown in Fig. 1.

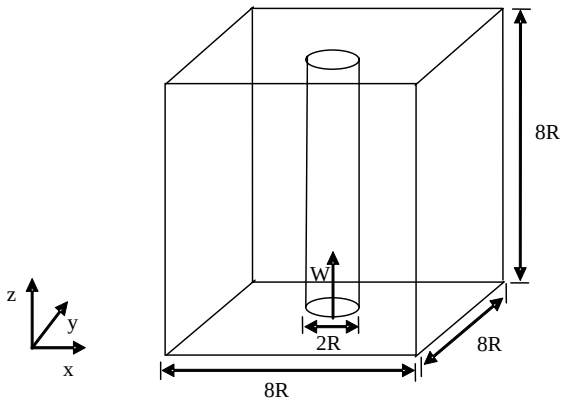

Figure 1. Scheme of computational domain.

The initial profile of axial velocity is the same in all simulations:

$$w_0(r,\theta,z,0)=\begin{cases}1 & (r\le R-\delta)\\ \frac{1}{2}\cdot\left[1-\tanh\left(\frac{r-R}{2\delta}\right)\right] & (R-\delta<r<R+\delta)\\ 0 & (r\ge R+\delta)\end{cases}, \tag{6}$$

where r is given by $r=\sqrt{x^2+y^2}$, with reference in the Cartesian system coordinate, R is the initial jet radius and δ is the characteristic half-width of the shear layer, equal to 2.5/16 m.

3. Simulations Results

3.1. Natural Jet

The "natural jet" is characterized for the imposition of a white noise inlet perturbation:

$$w(x,y,z,t)=w_0(x,y,z,0)+\left(\frac{0,5-a}{100,0}\right), \tag{7}$$

where *a* is a random number between 0 and 1.

a) Visualization of flow structures

Figure 2 presents the temporal evolution by means of the criterion Q isosurfaces in the 0.01 s^{-2} level.

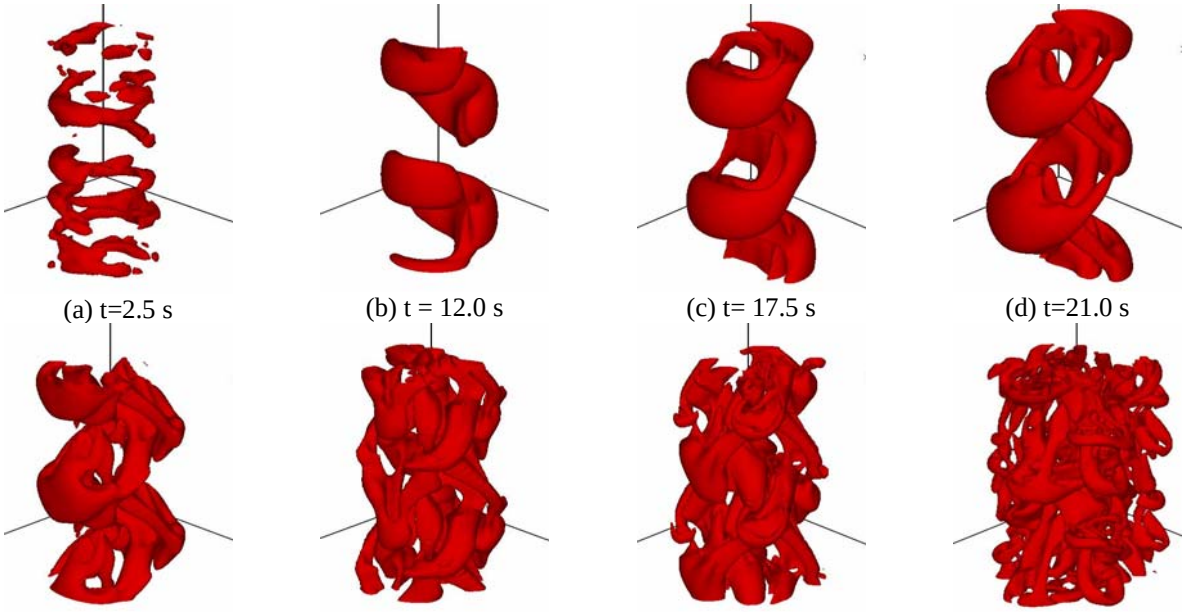

(a) t=2.5 s (b) t = 12.0 s (c) t= 17.5 s (d) t=21.0 s

(e) t = 22.5 s (f) t = 24.0 s (g) t = 26.0 s (h) t = 30.0 s

Figure 2. Criterion Q temporal evolution (Isosurface level = 0.01 s^{-2}): natural jet.

Figure 2(a) shows the remains of the random inlet perturbation. Fig. 2 (b) allows to verify the first instabilities. Figs. 2(c) and 2(d) show two consecutives rings that connect to each other, forming zigzag vortex structure, named alternated pairing (Urbin and Metais, 1997). These structures evolve (Figs. 2 (c), (d) and (e)). In Fig. 2 (e) it is possible to note the presence of spanwise filaments, which are formed by the vortex stretching. These filaments interact with the instabilities previously formed and a major interaction between the primary and secondary structures can be visualized since then. Turbulent flow is seen to develop from time t=26.0 s (Fig. 2(g)).

The alternated pairing vortices, evidenced in Fig 2(b), are typical structures of a natural jet, whose mechanism of formation was explained by Silva e Metais (2002). According to these authors, these alternated pairing is strongly

linked to the growth of the subharmonic mode. The primary vortex rings periodically shed at some distance from the nozzle with a distance L, their convection speed W_c and their preferred frequency f_p are related through $f_p=W_c/L$. The inlet perturbation creates different longitudinal frequency associated to with streamwise wavelength *2L*. It then induces an alternated radial shift of the vortex ring away form the jet axis. Due to the jet mean velocity profile, the outer part of the ring is then advected downstream at a speed which is lower than W_c, while the inner part is advected at a speed larger than W_c. The latter then tends to catch up the ring which was previously shed and this ultimately yields a localized pairing of the two consecutive rings.

The analysis above was made for a spatially developing jet, but many mechanisms are valid for the temporally developing jet. Actually, the temporal jet can be thought as a spatially-developing jet from a Lagrangian referential. The main difference is that in temporal jets there are not inlet and outlets, and then, the evolution of inlet perturbations is analyzed in the same space region.

Figures 3 and 4 show the vorticity field in temporal evolution in planes xz and xy, respectivelly.

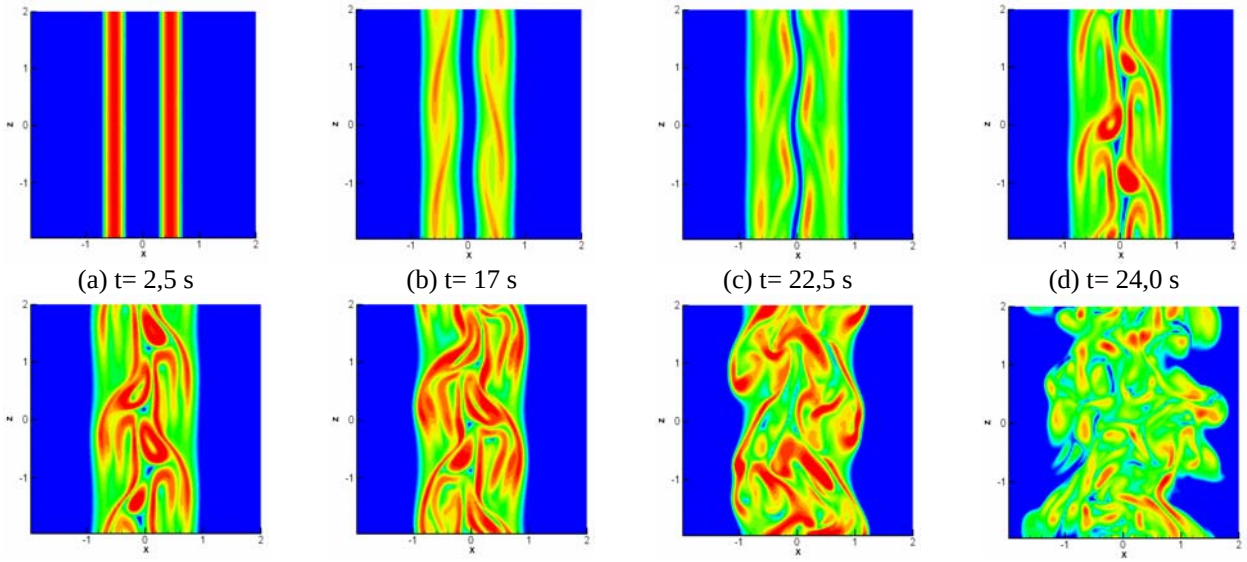

(a) t= 2,5 s (b) t= 17 s (c) t= 22,5 s (d) t= 24,0 s

(e) t= 26,0 s (f) t= 27,5 s (g) t= 30,0 s (f) t= 40,0 s

Figure 3. Vorticity $\|\vec{\omega}\|$ in temporal evolution in the plane xz (y=0): natural jet.

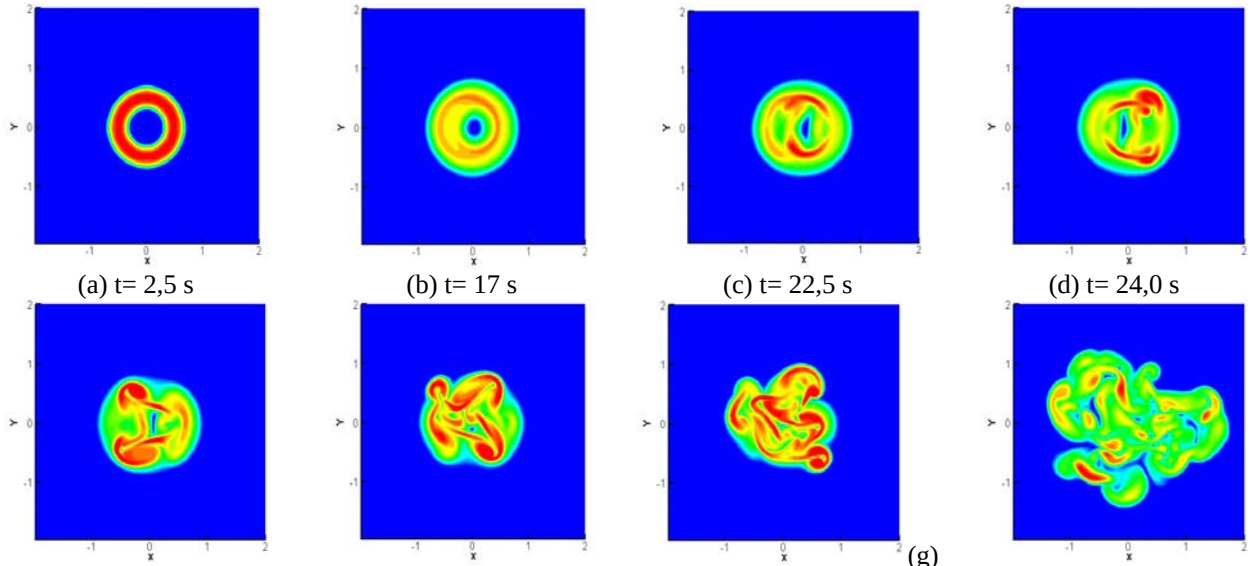

(a) t= 2,5 s (b) t= 17 s (c) t= 22,5 s (d) t= 24,0 s

(e) t= 26,0 s (f) t= 27,5 s (g) t= 30,0 s (h) t= 40,0 s

Figure 4. Vorticity $\|\vec{\omega}\|$ in temporal evolution in the plane xy (z=0): natural jet.

From Fig. 3, it can be seen that at the time t=2.5 s the flow does not present any instability. At t=17.0 s, the Kelvin-Helmholtz instabilities can be identified (Fig. 3(b) and Fig. 4(b)). These first instabilities develop in the following instants (Fig.3 (c-d) e Fig 4 (c-d)), and begin to interact with each other forming new vortex filaments, which can be observed in Figs. 3 (d-e) and in Figs. 4 (d-e). Figures 4 (e) and 4(f) show the counter-rotative vortices in the flow. The flow evolution from t= 27.5 s (Figs 3 (f) and 4 (f)) to t= 40.0 s (Figs 3 (h) e 4 (h)) is marked by a major interaction among the structures, with growing increase of system disorder and spanwise jet expansion.

b) Qualitative comparison to experimental data

The results obtained from the natural jet simulation were compared to experimental data from PIV measurements performed for a jet with a Reynolds number 1000 (Sakakibara, 2004). Figure 5 shows strict similarity between the structures in the simulation and experimental visualizations.

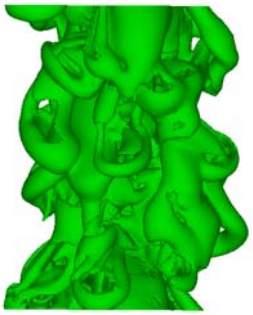

(a) Vorticity isosurface $\|\vec{\omega}\|$ =1.3s^{-1}

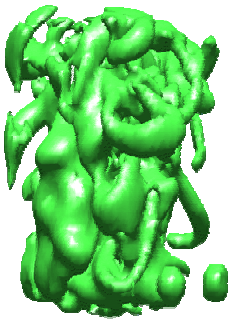

(b) PIV experimental measurements

Figure 5. Visualizations of structures in natural jet: (a) present work, (b) Sakakibara, 2004.

3.2. Bifurcating Jet

The bifurcating jet is resulted of the following inlet perturbations:

$$w(x,y,z) = w_0(x,y,z) + \left(\frac{0,5-a}{100,0}\right)\cdot e^{\left[-2\left(\frac{r-R}{2\delta}\right)^2\right]} \tag{8}$$

$$U_r = \left[0,01\cdot sin\left(2\pi\frac{z}{4,0}\right) + 0,02\cdot sin\left(2\pi\frac{z}{2,0}\right) + 0,03\cdot sin\left(2\pi\frac{z}{1,0}\right)\right]\cdot signal(\cos\theta) \tag{9}$$

The components of radial velocity are:

$$u = U_r\cos\theta\cdot e^{\left[-2,0\left(\frac{r-R}{2\delta}\right)^2\right]} \tag{10}$$

$$v = U_r\sin\theta\cdot e^{\left[-2,0\left(\frac{r-R}{2\delta}\right)^2\right]} \tag{11}$$

a) Visualization of flow structures

The Figure 6 presents the temporal evolution of the bifurcating jet through the Q criterion sosurfaces. The primary rings vortices showed at t=5.0s are folded in their middle along an axis perpendicular to the bifurcating plane. Moreover, strong streamwise vortices are seen to emerge from the crests of this azimuthal deformation (both upstream and downstream). It seems that the deformation imposed to the rings and the associated vortices leads to a fast three dimensionalization of the primary structures and longitudinal vortices leads to a fast three dimensionalization of the primary structures and therefore to this early transition turbulence. Indeed, once the primary vortex rings are deformed by the imposed excitation, the two parts of the folded ring tend to travel in opposite directions due to their self-induced velocity. This mechanism explains the significant increase of the spreading rate in the bifurcating plane.

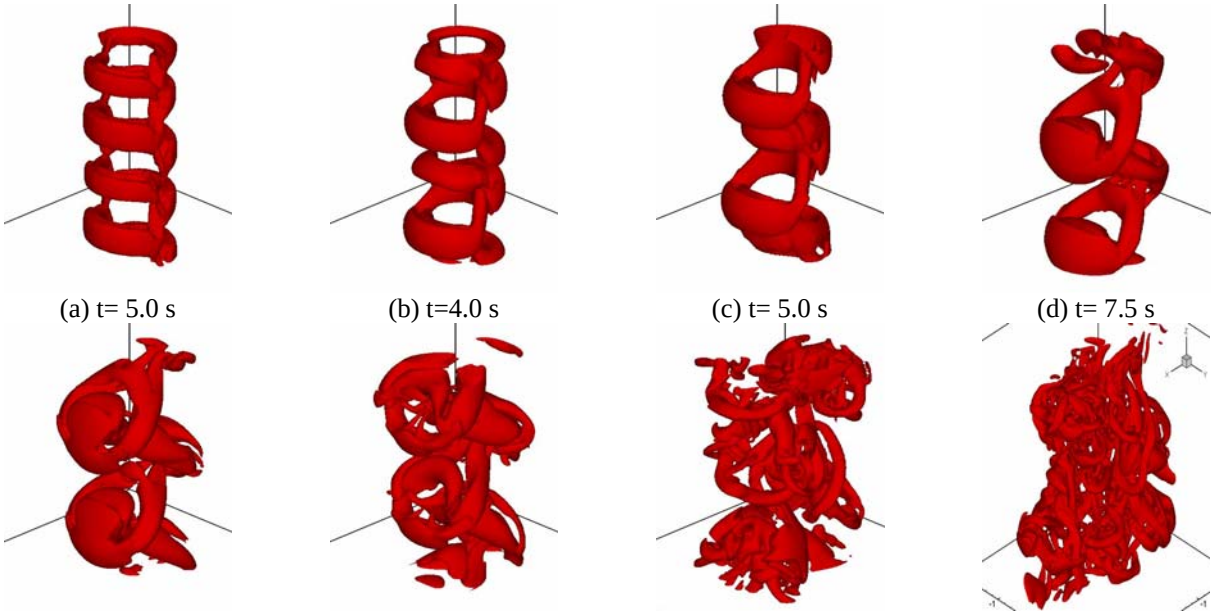

(a) t= 5.0 s (b) t=4.0 s (c) t= 5.0 s (d) t= 7.5 s

(e) t= 9.0 s (f) t= 10.0 s (g) t= 12.5 s (h) t= 20.0 s

Figure 6. Criterion Q temporal evolution (Isosurface Level 0.1 s^{-2}): bifurcating jet.

The Figures 7 and 8 show the temporal evolution of vorticity in the planes xz e xy, respectivally. It is possible to verify the quick transition to turbulence, as well as the great spreading rate in spanwise direction x, which can be observed especially on Fig. 8. The preferential jet expansion in spanwise direction x is a consequence of the multiplication of the signal of $\cos\theta$ to the radial perturbation, which leads to the alternated shift of primary structures in opposite directions (bifurcation of the jet).

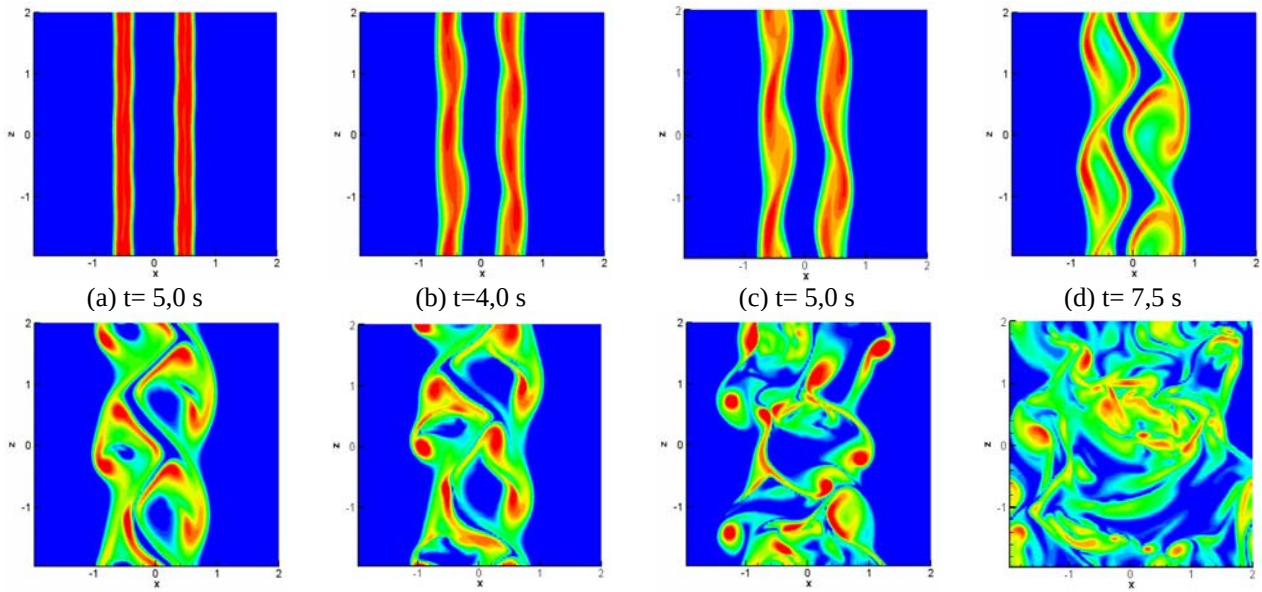

(a) t= 5,0 s (b) t=4,0 s (c) t= 5,0 s (d) t= 7,5 s

(e) t= 9,0 s (f) t= 10,0 s (g) t= 12,5 s (h) t= 20,0 s

Figure 7. Vorticity $\|\vec{\omega}\|$ temporal evolution in the plan xz (y=0): bifurcating Jet.

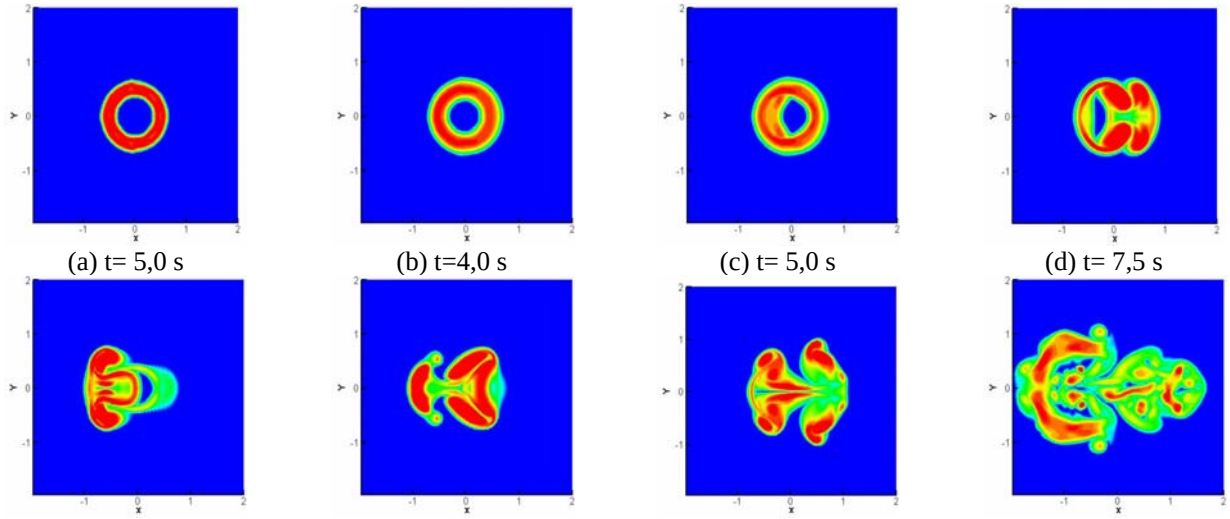

(a) t= 5,0 s (b) t=4,0 s (c) t= 5,0 s (d) t= 7,5 s

(e) t= 9,0 s (f) t= 10,0 s (g) t= 12,5 s (h) t= 20,0 s

Figure 8. Vorticity $\|\vec{\omega}\|$ temporal evolution in the plane xy (z=0): bifurcating jet.

3.3. Comparison between Natural and Bifurcating Jets

Figure 9 allows the comparison between the evolution of the natural and bifurcating jets studied in the present work. It is possible to note that the transition to turbulence is really faster in the bifurcating jet, as already commented. In the bifurcating jet, the rings form more quickly and spread more in the spanwise direction x. The bifurcating jet expansion in direction x is considerable at t=20.0 s, while the natural jet presents a least expressive expansion, even at t=30.0 s. This comparison suggests the possibility of jet control in spatial development through the imposition of different kinds of perturbation to the initial conditions.

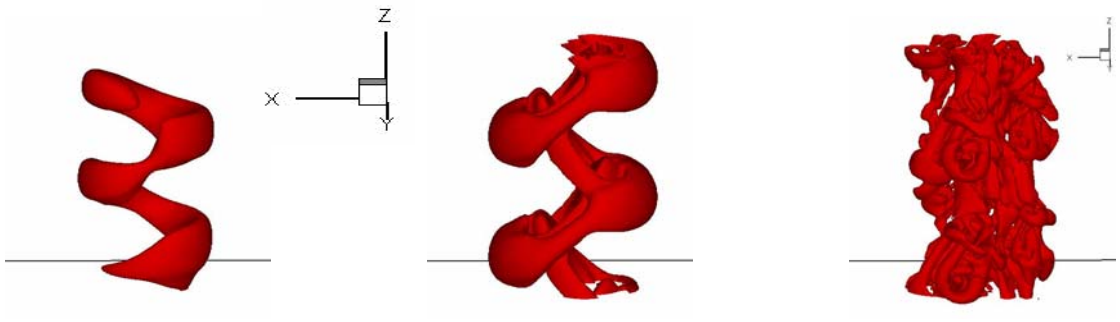

t= 5,0s t=20,0 s t= 30,0s

a) Criterion Q isosurfaces (level = 0.01 s^{-2}): natural jet

t= 5,0s t=10,0 s t= 20,0s

b) Criterion Q isosurfaces (level= 0.1 s^{-2}): bifurcating jet

Figure 9. Comparison of temporal evolution trough criterion Q isosurfaces between Natural and bifurcating jets.

The spectrum of turbulent kinetic energy for the natural and bifurcating jets are showed at different instants of time in Fig. 10.

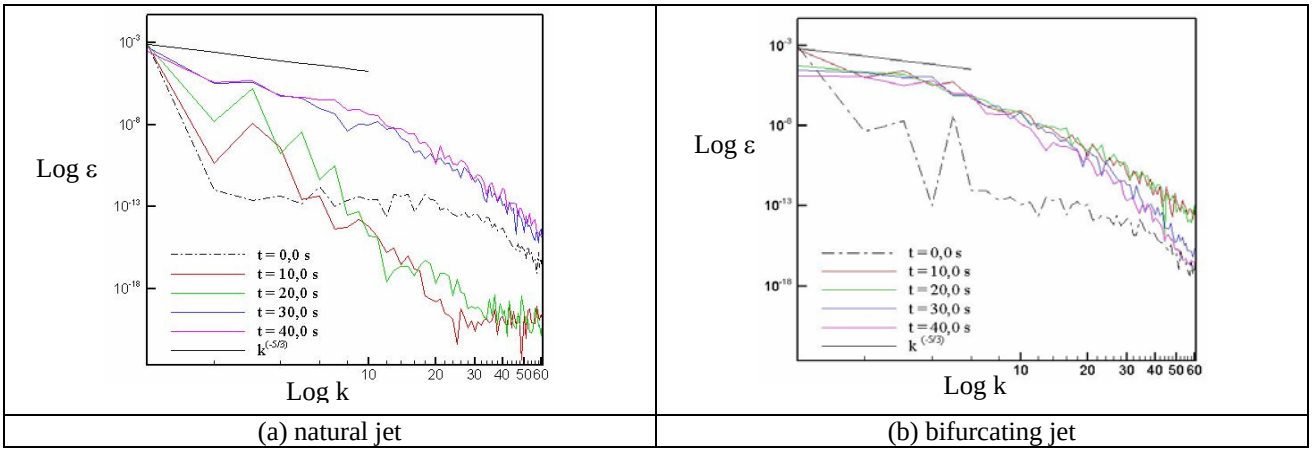

(a) natural jet (b) bifurcating jet

Figure 10. Turbulent Kinetic Energy Spectrum for natural and bifurcating Jets.

It is possible to verify that the energy spectrum of the natural jet in the range log(k)=3 to log(k)=10 approach the inclination of -5/3 as time evolves. Therefore, the completely developed turbulent flow is reached in the time range studied. From log(k)=10 on, the decay of kinetic turbulent energy can be identified, which is expected for the free jet in temporal development. For the bifurcating jet it is possible to identify the proximity of the inertial region to the inclination of -5/3 in the range log k=3 to 5. From log k=5 on, the energy decay is seen to start.

4. References

Crow, S.C. and Champagne, F.H., 1971, "Orderly structure in jet turbulence", Journal Fluid Mechanics, 48, 547.

Gutmark, E.J. and Grinstein, F.F., 1999, "Flow control with noncircular jets", Annu. Rev. Fluid Mech., 31, 239.

Narasimha, R.1990, "The utilities and drawbacks of traditional approaches". In Whither Turbulence. Turbulence at the crossroads (ed. J.L.Lumley), pp.12-48. Springer.

Silva, C.B. and Métais, O., 2002. "Vortex control of bifurcating jets: A numerical study." Physics of Fluids, 2002, Vol. 14, n. 11, pp. 3798-3818.

Suzuki, H., Kasagi, N, and Suzuki, Y., 2000. "Active control of an axisymmetric jet with an intelligent nozzle", 1st Symposium on Turbulent Shear Flow Phenomena.

Townsend, A.A., 1976, "The Structure of Turbulent Shear Flow" Cambridge Univesity Press.

Zaman, K.B.M.Q. and Hussain, A.K.M.F., 1980, "Vortex pairing in circular jet under controlled excitation. Part 1. General jet response", Journal of Fluid Mechanics 101, 449.

Zaman, K.B.M.Q., Reeder, M.F. and Samimy, M., 1994, "Control of an axisymmetric jet using vortex actuators", Physics Fluids 6, 778.

5. Responsibility notice

The authors are the only responsible for the printed material included in this paper.